

A wave modelling study of the 1998 Sydney to Hobart yacht race

D.J.M. Greenslade

Bureau of Meteorology Research Centre, Australia

(Manuscript received January 2000; revised August 2000)

The 1998 Sydney to Hobart yacht race was the most disastrous event in any offshore race held in Australian waters. During the afternoon of 27 December, the fleet encountered a severe storm off the coast of southern New South Wales that caused the abandonment of five yachts and forced a further 66 boats to retire from the race. The aim of this paper is to provide a description of the evolution and subsequent development of the sea-state during the storm. A high-resolution 0.1° wave model forced by high-quality wind fields has been run over the Bass Strait region for a 36-hour period during the yacht race (11pm 26 December to 11am 28 December). Wind forcing fields were obtained from the lowest level of a very high-resolution (0.05°) atmospheric model. The significant wave height (SWH) in the race region is found to be high throughout most of the time period with a maximum SWH of 8.5 m, east of Gabo Island during the evening of 27 December. The predominant wave direction is towards the northeast, however, the existence of westerly propagating swell, forced by an earlier storm in the Tasman Sea contributes to confused seas in this region. The wave model compares qualitatively very well with observations of SWH at Kingfish B platform in Bass Strait. Possible sources of error in SWH include the lack of current or depth refraction in the model, remaining errors in the surface wind fields, and the omission of 'gustiness' in the wave growth term within the wave model.

Introduction

The 1998 Sydney to Hobart yacht race was the most disastrous event in the race's 54-year history, and indeed of any offshore race in Australian waters. Of the 115 yachts departing Sydney Harbour at 1pm on 26 December*, only 44 reached their destination. During the afternoon of 27 December, the fleet encountered a severe storm off the coast of southern

New South Wales (NSW) which caused the abandonment of several yachts and the death of six people. Five boats were sunk and a further sixty-six boats retired from the race. Fifty-five people were rescued in the biggest maritime rescue operation ever undertaken in Australian waters (Cruising Yacht Club of Australia 1999, hereafter CYC99).

Figure 1 shows a map of the race region with a few depth contours outlined. The thick line on this figure represents the trajectory taken by one of the 44 yachts to finish the race. It can be seen that after reaching Gabo Island, the yacht was subsequently blown off

Corresponding author address: D.J.M. Greenslade, Bureau of Meteorology Research Centre, GPO Box 1289K, Melbourne, Vic. 3001, Australia.

* Local times are Eastern Australian Daylight Saving Time (EADST) or UTC + 11 hours.

course by the storm. Also marked on the map is Kingfish B platform (KFB), from which marine observations were available.

The aim of this paper is to provide a description of the evolving sea-state during the yacht race. There is no attempt to examine the accuracy of the forecasts and warnings issued by the Bureau of Meteorology. This has been presented elsewhere (see, for example, National Meteorological Operations Centre (1998) or Bureau of Meteorology (1999)). Firstly, the wave model and wind forcing fields used for this study are described, followed by a presentation of the modelled wave fields, along with a discussion of some potentially important factors governing the development of the sea state. Then, the surface winds and wave model results are compared with the available observations and possible causes for discrepancies are discussed, followed by the conclusions.

Description of the wave model

The wave model used for this study is a high-resolution version of the wave model, WAM. The WAM model (Komen et al. 1994) is a third-generation wave model, i.e., the wave transport equation is solved explicitly without assuming a form for the evolving wave spectrum. The wave transport equation is:

$$\frac{\partial F}{\partial t} + \nabla(c_g F) = S_{in} + S_{nl} + S_d + S_{bot} \quad \dots 1$$

where F is the wave spectrum, c_g is the group velocity and the terms on the right-hand side represent the source terms: S_{in} is the energy input due to wind forcing, S_{nl} the non-linear energy transfer between groups of resonant waves, S_d the dissipation of energy due to whitecapping, and S_{bot} the dissipation of energy due to bottom friction. The WAM model is implemented operationally at many forecasting centres around the world, including a version at the Australian Bureau of Meteorology (AUSWAM).

AUSWAM currently comprises a global model at 3° spatial resolution, a regional model at 1° resolution and a mesoscale model at 0.25° resolution. The mesoscale model is nested inside the regional model, which is in turn nested inside the global model. The regional model spans the oceans around Australia and covers an area from 60°S to 12°N and from 69°E to 180°. The mesoscale model covers the southeast of Australia and ranges from 50°S to 24°S and from 126°E to 164°E.

For the global and regional models the source terms are integrated every 10 minutes and the propagation terms every 20 minutes, while for the mesoscale model, the timestep is five minutes for both source and

propagation terms. In terms of the wave spectrum, the directional resolution is 30° and there are 25 frequency bins ranging from 0.0418 Hz to 0.4114 Hz. This represents wave periods from approximately 24 seconds to 2.5 seconds. At spatial resolutions of 1° or greater, very few of the wave model grid-points are in water depths of less than 100 m and so the regional and global wave models are run with deep-water physics only, while the mesoscale model includes shallow-water physics. The global and regional versions include the assimilation of significant wave height (SWH) data from the ERS-2 altimeter (Greenlade 2001). Major differences between AUSWAM and other versions of WAM are that the deep-water versions of AUSWAM are run with third-order propagation numerics and enhanced wave dissipation (Bender 1996).

Winds used to force AUSWAM are 10 m surface wind velocities obtained from the Bureau of Meteorology's operational global, regional and mesoscale atmospheric models, GASP (Seaman et al. 1995), LAPS (Puri et al. 1998) and MESO_LAPS (National Meteorological and Operations Centre 1999), respectively. The 10 m surface winds are obtained from the lowest levels of the atmospheric models via Monin-Obukhov theory with empirical stability functions (Garratt 1992).

When compared to *in situ* observations of significant wave height (SWH) around the Australian coast, the root mean square (rms) error of hindcast SWH from the regional wave model is approximately 0.4 m with a Scatter Index (SI) of approximately 0.25. The SI for modelled SWH is a measure of the time (or space) varying errors and is defined as the ratio of standard deviation of error to the mean observed SWH. It is given by

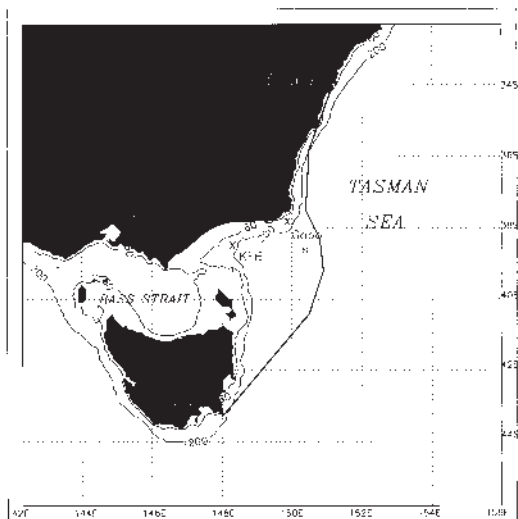
$$SI = \frac{\sqrt{\frac{1}{N} \sum_{i=1}^N (SWH_m^i - SWH_o^i - bias)^2}}{\frac{1}{N} \sum_{i=1}^N (SWH_o^i)} \quad \dots 2$$

where SWH_m is modelled SWH, SWH_o is observed SWH and N is the number of observations.

Model configuration

For this particular study, some details of the wave model's configuration were altered. The spatial domain is centred on Bass Strait and ranges from 45°S to 33°S and from 143°E to 155°E (see Fig. 1). Although most of the domain is more than 200 m deep, the depth throughout Bass Strait is less than 85 m, indicating that shallow water effects will be important in this area. The 0.1° bathymetry used for this study was obtained from a 30 arc-second bathymetric dataset of the Australian continental shelf produced by

Fig. 1 Map showing the area of the Sydney to Hobart yacht race. 60 m and 200 m bathymetric depth contours are marked. The thick black line shows the trajectory taken by one of the yachts to complete the race.



the Australian Geological Survey Organisation. The spatial resolution of the wave model was increased to 0.1° , or approximately 10 km. The source terms and propagation terms were integrated every five minutes. In terms of the wave spectrum, the directional resolution was increased to 15° while the frequency resolution remained the same as in the operational models. Fields of SWH, mean wave direction and other diagnostic variables are output every hour.

Wind forcing

It is generally acknowledged that most of the errors in wave prediction fields arise from errors in the wind forcing fields (Cardone et al. 1996; Komen and Smith 1999). Therefore, for a detailed wave modelling study, it is desirable to obtain the best possible surface wind fields. In this case, they were provided by a very high resolution (0.05°) atmospheric model described in Mills (2000) and Mills (2001). Mills (2000) shows that the hindcast is of very high quality, and we can be confident that the surface wind fields obtained from this atmospheric model are a good representation of the true conditions. This assertion will be examined more closely later in this paper.

New wind forcing fields were provided at hourly intervals. The lowest level of the atmospheric model was very close to 10 m and the 10 m winds were obtained in a similar way as for the operational models. Since the spatial resolution of the atmospheric

model is simply twice the spatial resolution of the wave model, no interpolation of the wind fields to the wave model grid was necessary. Surface wind fields are not presented here, but the general synoptic situation was as follows.

A cold front passed through the region during the morning of 26 December, prior to the start of the yacht race. A low pressure system formed within Bass Strait during 26 December, became cut-off at about midnight and continued to move eastwards. A small-scale secondary low developed over northern Tasmania in the early morning of 27 December, and rapidly intensified, with a band of very strong westerly winds on its northern side. It was these strong winds and the waves forced by these winds that contributed to major problems for the race fleet. A detailed description of the meteorological situation can be found in Mills (2001).

Boundary and initial conditions

To obtain boundary conditions for the Bass Strait model it was necessary to rerun the global and regional wave models with increased spectral resolution. These were forced with operational hindcast winds. The regional model provided wave spectra at 1° intervals along the edges of the high-resolution grid to use as boundary conditions.

To initialise the wave model for a cold start, wave spectra with a prescribed form, JONSWAP spectra (Hasselmann et al. 1973), were defined at each model grid-point from the local initial winds according to fetch laws with a \cos^2 directional distribution (Gunther et al. 1992). In this case, an initial fetch of 30 km was imposed at all grid-points. This ensured that some swell energy was present in the model at the beginning of the spin-up period. Initialisation for all three domains (global, regional and Bass Strait) occurred at 11 am 20 December and the models were spun up for approximately 6.5 days, using the operational hindcast surface winds as forcing fields. After the initial spin-up period, the model was then run for 36 hours over the time period of interest, from 11 pm 26 December, until 11 am 28 December.

Evolution of SWH field

The predominant influence on the sea-state at any time is the local wind forcing, however there are other important elements that must be taken into consideration. In this section, three factors affecting the development of the sea-state during the yacht race are considered: (a) the wave conditions in the Tasman Sea, i.e., the area surrounding the race region; (b) the East Australian Current system; and (c) the local wind forcing.

Tasman Sea

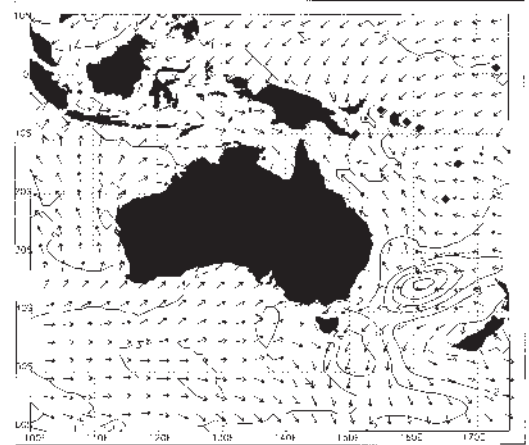
We first consider the wave conditions of the area surrounding the race region for the time period leading up to the yacht race. Figure 2 shows the SWH field obtained from the regional wave model at 11 am 26 December, a few hours before the commencement of the race. Note that only a portion of the regional model domain is shown here. This figure shows that a region of high SWH has developed in the Tasman Sea, at around (160°E, 35°S) caused by strong winds associated with a low-pressure system in this area. The maximum SWH at this time is greater than 6 m. The arrows on this plot represent the mean wave direction at every third model grid-point. The mean wave direction is defined as the energy-weighted average direction of all spectral wave components. This means that if there is more than one wave system present, there may be no waves actually propagating in the 'mean' direction. However, inspection of the directional wave spectrum near the peak of this storm indicates that the vast majority of the wave energy here is propagating towards the west, with only a small directional spread.

During 27 December, this area of strong winds and high SWH moves southward, while the mean wave direction turns towards the southwest. Although the area of maximum SWH remains some distance away from Bass Strait, this storm still has a significant influence over the sea-state near the coast. During the period of the yacht race, swell with a period of approximately 11 seconds propagates towards the Australian coast and into the race region.

East Australian Current

Another potentially important factor governing the development of the sea state in the area is the East Australia Current (EAC). The EAC is a western boundary current carrying warm water from the Coral Sea southwards along the east coast of Australia. Eddies pinch off from the meanders of the EAC and the current speeds at the edge of these eddies can be up to 2 m/s (Andrews and Scully-Power 1976). Although no direct *in situ* measurements of the velocity field of the EAC are available for the time period of the yacht race, it is possible to estimate geostrophic surface currents from satellite altimeter measurements of relative sea-surface height. Figure 3 shows surface velocities estimated from combined ERS-2 and Topex/Poseidon sea-surface height data during a 15-day time window centred on 30 December. It should be noted that in depths of less than approximately 1000 m, errors in correcting the observed sea-surface height for tides are too large for reliable estimates of surface currents to be made. Therefore the currents within Bass Strait are unlikely to be accurate.

Fig. 2 SWH (m) and mean wave directions from the regional wave model at 11am 26 December, just before the start of the yacht race. An area of high SWH is present in the Tasman Sea at around (160°E, 35°S), and the mean wave directions indicate that these waves are propagating towards the Australian coast.

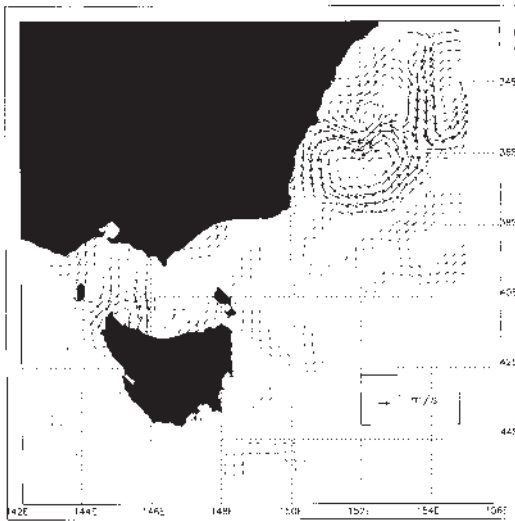


It can be seen that during this time period, there was a large anti-cyclonic eddy centred at about (152°E, 36.5°S). There are strong currents around the boundary of this eddy with speeds of up to 2 m/s. Note in particular an eastward-flowing current at around 37.5°S. Images of sea-surface temperature from infrared sensors aboard NOAA satellites confirm this diagnosis for the time period of the yacht race (G. Cresswell, personal communication).

The effect of an adverse current on a wave field is to decrease the wavelength and increase the SWH. This therefore has the effect of steepening the waves, although the amount by which the waves are altered is uncertain. Previous studies have suggested that the SWH can be increased by up to 50 per cent in extreme cases although it is more likely to be closer to 10 per cent (Komen et al. 1994). The eastward flowing current described above will therefore cause the westerly propagating swell (from the Tasman Sea storm) to steepen.

It is currently not feasible to include the effect of surface currents in an operational wave model due to the difficulty in obtaining observed or modelled surface currents in real time. This situation may be improved with the implementation of projects such as the Global Ocean Observing System (GOOS) or the Global Ocean Data Assimilation Experiment (GODAE) (Swail et al. 1999).

Fig. 3 Surface geostrophic currents from satellite altimetry for a 15-day time period centred on 30 December.



Sea-state development

Figure 4 shows a three-hourly time series of SWH fields from the high resolution Bass Strait wave model during the time period of interest. In the initial wave field (Fig. 4(a)), the SWH over most of the domain is 2 m to 4 m. The highest SWH occurs near the eastern boundary of the grid. This represents the swell that is propagating into the region from the Tasman Sea storm described previously.

During the next 12 hours, it is possible to see the signature of the passage of the cold front in the mean directions of the waves. There is a clear distinction (e.g., in Fig. 4(c) at 5 am 27 December) between the waves propagating generally towards the southwest and waves propagating towards the east. The mean wave directions take some time to adjust to the change in wind direction. The position of the 'front' in Fig. 4(c) occurred in the wind field at 1 am, i.e. 4 hours earlier.

After the front has swept through the Bass Strait region, the SWH in the western half of Bass Strait increases significantly, reaching a maximum of over 8 m, just south of Melbourne at 11 am. The mean wave direction here at this stage is towards the north, and during the afternoon of 27 December, the SWH in the western half of Bass Strait abates somewhat.

The strong westerly winds associated with the small-scale secondary low pressure system over northern Tasmania cause a build-up in SWH in the eastern half of Bass Strait and by 2 pm 27 December (Fig.

4(f)), the SWH off the coast of southern NSW is over 6 m. By this time the passage of the low-pressure system has caused winds over most of Bass Strait to strengthen and swing to the southwest and this causes the SWH off Gabo Island to increase further. By 11 pm, the peak SWH has started to move slightly offshore and a maximum SWH of 8.5 m is reached between 10 pm and 1 am. During the early hours of the 28th, the area of peak SWH continues to move off into the Tasman Sea. SWH in the race region, southeast of Gabo Island remains fairly high at approximately 5 m.

A comparison of the times and locations where several of the yachts capsized (CYC99) (Fig. 5) with the time series of SWH (Fig. 4) shows that the problems for the yachts occurred close to the area of highest SWH. However, another important consideration is the fact that multiple wave systems were present here. In particular, the easterly propagating wave systems created by the strong westerly winds combined with the westerly propagating swell arising from the earlier Tasman Sea storm, possibly steepened by the EAC. These multiple wave systems can be seen in a plot of the directional wave spectrum in Fig. 6(a). This spectrum is representative of the sea-state at a time and location close to the point where the yacht *Business Post Naiad* was rolled (see Fig. 5). Figure 6(b) shows the directional average of this spectrum. Note that the mean wave direction here is 68° , i.e., towards east-northeast. This is not representative of the actual sea state, as the directional wave spectrum shows there is also a large amount of wave energy propagating towards the west.

The term 'crossing seas' or a 'confused sea' is used to describe the situation in which wave systems propagating in more than one distinct direction are present in a wave field. The existence of large waves propagating in many different directions causes the water surface to become highly irregular. These large, steep and chaotic waves can thus become hazardous to marine vessels. In addition, the situation depicted in Fig. 6(a) shows that the two wave systems are propagating in almost opposite directions. Although the predominant wave direction is towards the east (the eastward peak has a higher spectral density), single waves propagating in the opposite direction will occasionally appear. These individual waves are sometimes termed 'rogue waves' (Torum and Gudmestad 1990).

Comparison with observations

There are few reliable observations of SWH available in this area at this time - a reflection of the general difficulty in obtaining *in situ* marine observations. The locations of the ERS-2 and Topex/Poseidon satellite overpasses in this short time

Fig. 4 SWH (m) from the high-resolution wave model at three-hourly intervals. White arrows show mean wave directions. (a) 11 pm 26 December; (b) 2 am 27 December; (c) 5 am 27 December; (d) 8 am 27 December; (e) 11 am 27 December; (f) 2 pm 27 December; (g) 5 pm 27 December; (h) 8 pm 27 December; (i) 11 pm 27 December; (j) 2 am 28 December; (k) 5 am 28 December; (l) 8 am 28 December.

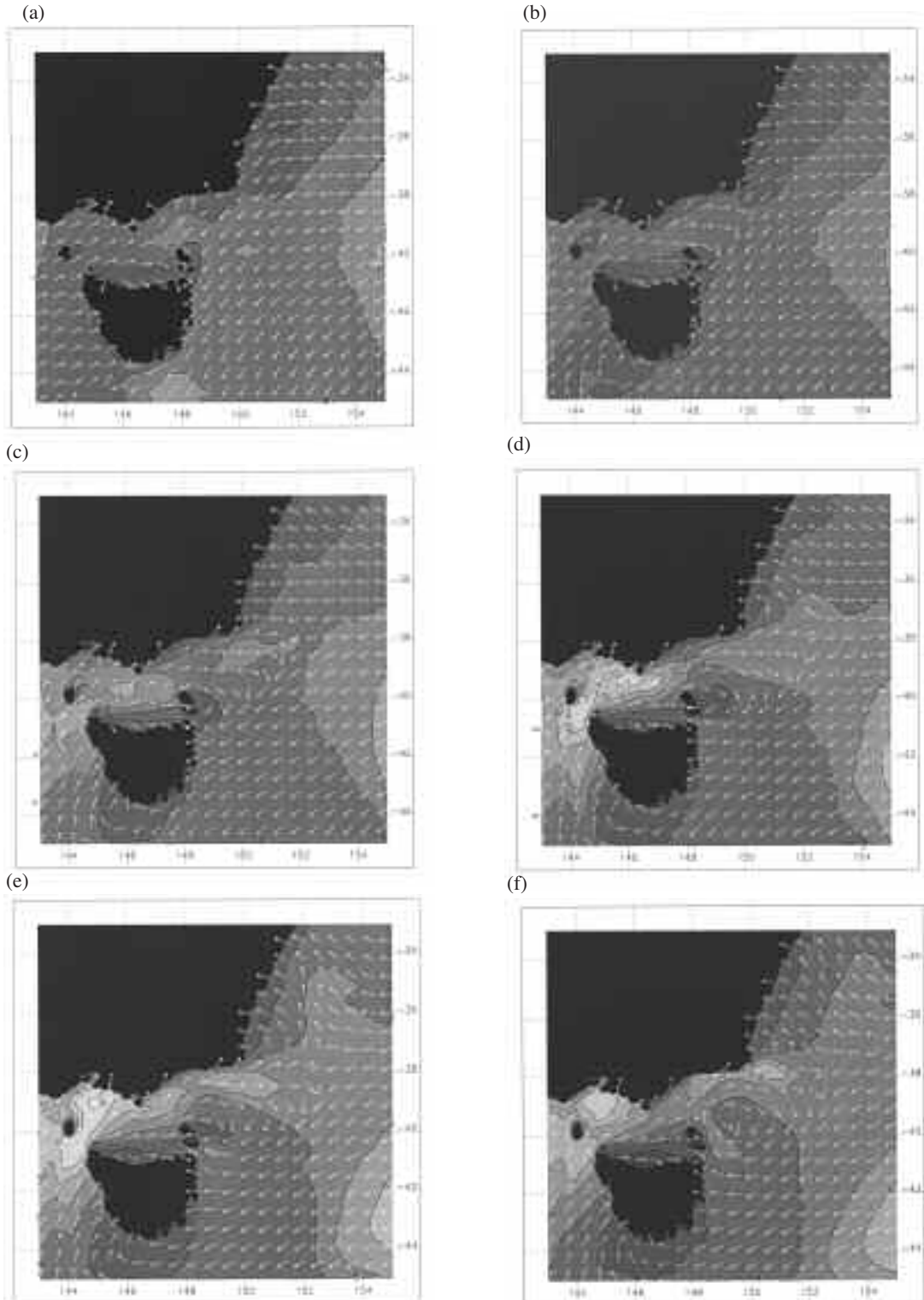
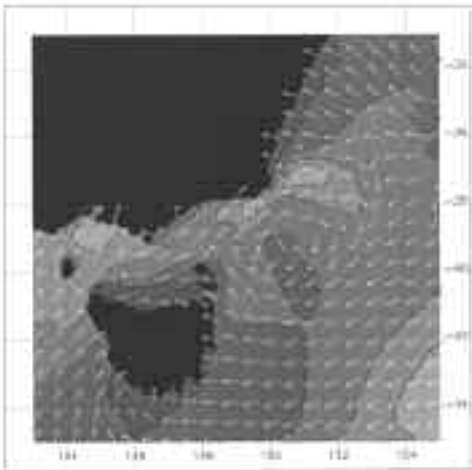
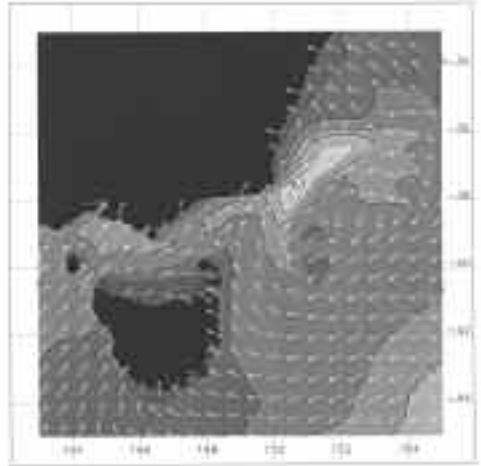


Fig. 4 Continued.

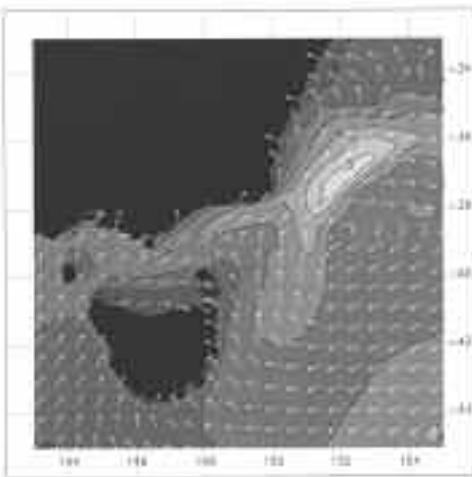
(g)



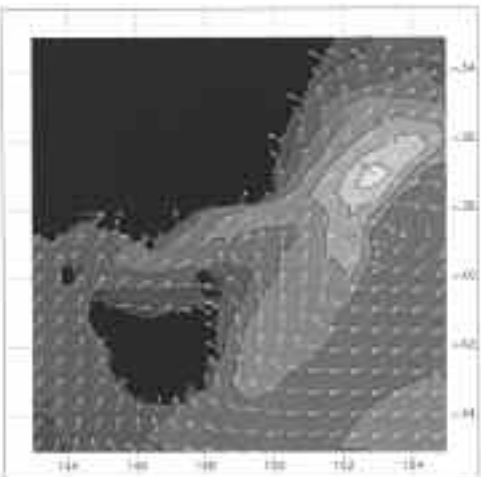
(h)



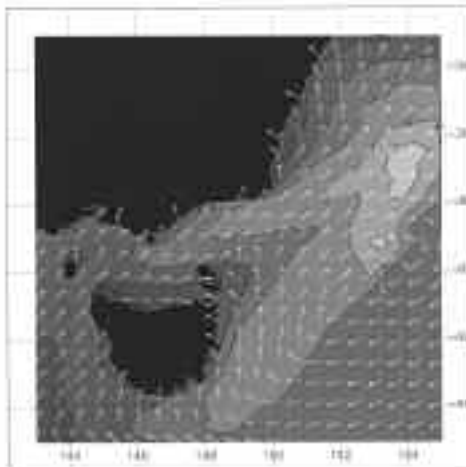
(i)



(j)



(k)



(l)

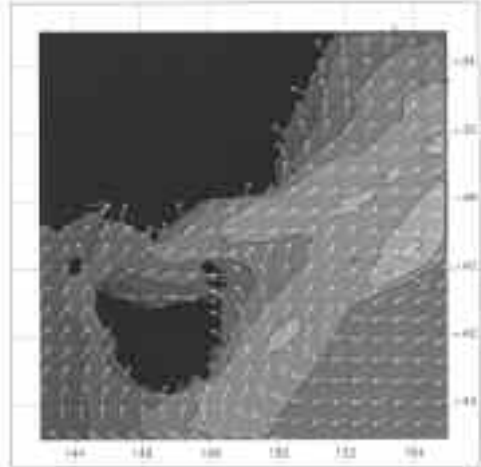
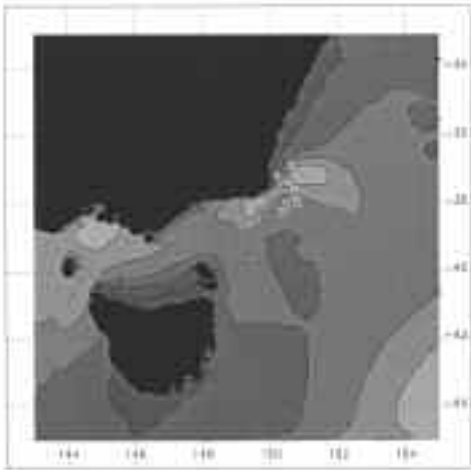


Fig. 5 Contours of SWH (m) from the high-resolution wave model at 5 pm 27 December. The white numbers show the approximate locations where several of the competing yachts capsized or were dismantled. 1: *Mintata* 2:15 pm, 2: *Stand Aside* 4 pm, 3: *Sword of Orion* 4:50 pm, 4: *Winston Churchill* 5 pm, 5: *Business Post Naiad* 5:20 pm, 6: *Kingurra* 6:30 pm.

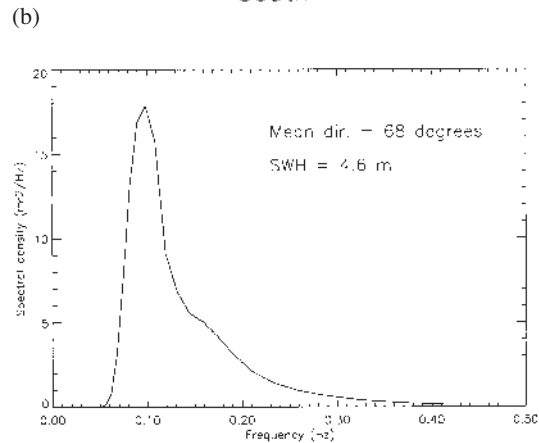
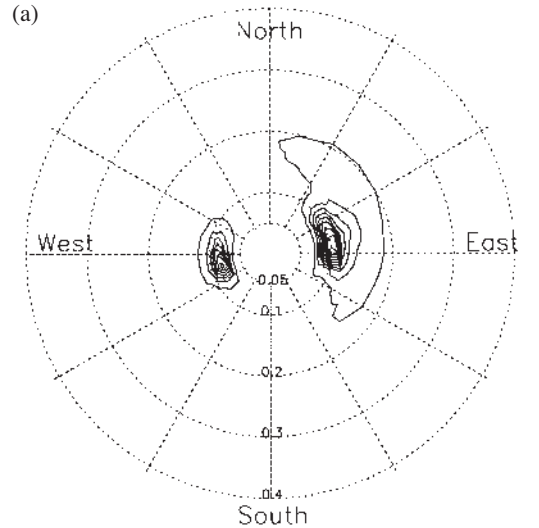


period unfortunately do not coincide with the area of interest. We concentrate here on the data available from KFB at (148.2°E, 38.6°S) in Bass Strait (see Fig. 1). In addition, some reports from the yacht fleet are considered. These, however, are subjective visual observations and are therefore less reliable than instrumented measurements.

Surface winds

We first consider the accuracy of the forcing fields and compare the surface winds obtained from the atmospheric model with the observed winds at KFB. Wind speeds were measured by an anemometer mounted 44 m above the sea surface on the KFB platform. These winds need to be extrapolated to a height of 10 m to enable comparison with the 10 m surface winds used to force the wave model. In neutrally stable conditions, a logarithmic wind profile applies. In this particular situation, air and water temperature measurements from KFB show that after the passage of the cold front on 26 December, the water was several degrees warmer than the air, resulting in low static stability. This is likely to contribute to deviations from a logarithmic wind profile. The following analysis can nevertheless provide a useful assessment of any major differences occurring between the modelled and observed surface winds.

Fig. 6 (a) Directional wave spectrum (m²/Hz) from the wave model at (150°E, 38.1°S) at 5 pm 27 December. The peak on the 'east' axis represents waves propagating towards the east. (b) Directional average of the spectrum shown in (a). This spectrum is representative of the sea state close to the time and location where the yacht *Business Post Naiad* was rolled.



So, assuming a logarithmic wind profile:

$$\frac{\partial u(z)}{\partial z} = \frac{u_*}{\kappa z} \quad \dots 3$$

where $u(z)$ is wind speed at height z above the sea-surface, u_* is friction velocity and κ is von Karman's constant ($= 0.41$), wind speed at 44 m can therefore be converted to wind speed at 10 m via:

$$u(10) = u(44) - \frac{u_*}{\kappa} \ln\left(\frac{44}{10}\right) \quad \dots 4$$

Using the drag law $u_*^2 = C_D u(10)^2$, we find:

$$u(10) = \frac{u(44)}{1 + \frac{\sqrt{C_D}}{\kappa} \ln\left(\frac{44}{10}\right)} \quad \dots 5$$

The fact that C_D is itself a function of 10 m wind speed again complicates these calculations, but a more detailed examination of the structure of the surface boundary layer is outside the scope of this paper. Here, C_D is taken to be 0.0015, which is an appropriate value for a 10 m wind speed of approximately 15 m/s (Large and Pond 1981).

Figure 7(a) shows a comparison of 10m wind speed from the atmospheric model at the location of KFB, the wind speed measured at the anemometer, and the measured wind speed extrapolated to 10 m. Validation statistics are shown in the first row of Table 1.

Table 1. Validation statistics for surface winds and SWH when compared to observations at KFB.

	<i>Bias</i>	<i>R</i>	<i>rms</i>	<i>SI</i>
u_{10} (KFB)	-1.3 m/s	0.58	3.6 m/s	0.23
u_{10} (pt2)	-1.3 m/s	0.86	2.7 m/s	0.16
SWH (pt2)	-0.34 m	0.93	0.68 m	0.16

Here, bias is (observed - modelled), rms is the root-mean square difference, SI is the Scatter Index (see Eqn 2) and R is the linear correlation coefficient.

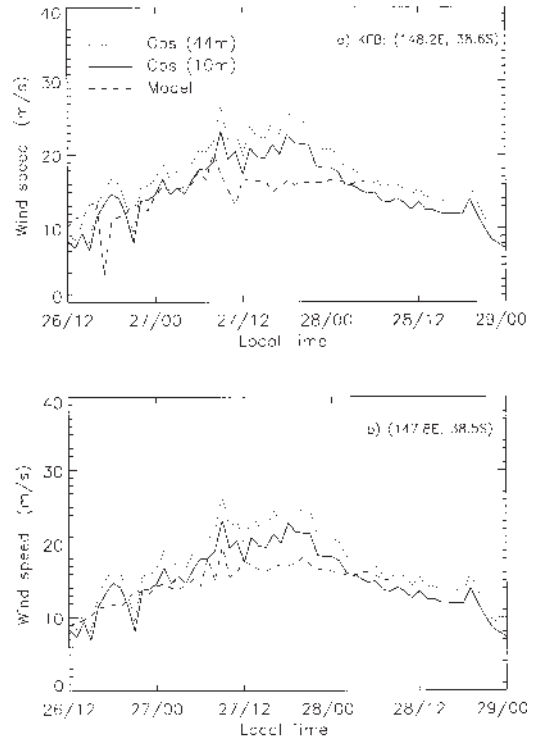
The relatively poor match between modelled and observed wind speeds at KFB could be because the assumption of neutral stability is not appropriate in this situation. However, there is also the possibility that the small-scale features of the wind field are simply slightly displaced in the model. Upon inspection of the modelled winds from the surrounding grid-points, it was found that the best correlation with the observations occurred at (147.8°E, 38.5°S). The 10m wind speed from this location (pt2) is shown in Fig. 7(b) and the validation statistics are also shown in Table 1.

It can be seen that although the bias is the same, there is a much greater correlation between the modelled and observed winds at this second location. This suggests that the small-scale characteristics of the wind forcing fields may be displaced slightly to the west in the atmospheric model. Following this implication, comparisons between modelled wave fields and KFB observations were performed using wave model output at this second location.

Significant wave height

Figure 8 shows a comparison between hourly SWH measured by a wave sensor at KFB and the SWH generated by the high-resolution wave model at pt2.

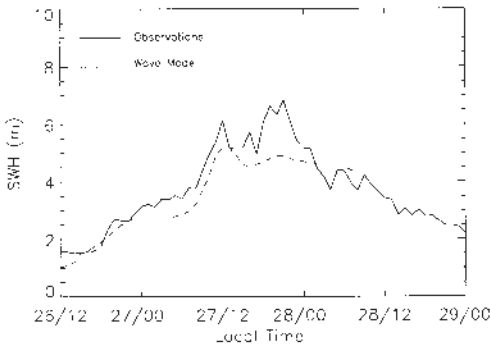
Fig. 7 (a) Comparison between 10 m wind speed from the atmospheric model (dashed line) and wind speed measured by a 44 m high anemometer at Kingfish B platform (dotted line). The solid line shows the observations extrapolated to 10 m assuming a logarithmic wind profile. (b) The same as (a) but modelled wind speeds are at (147.8°E, 38.5°S).



Overall, there is good phase agreement between the modelled SWH and the data. The rapid increase during 27 December is represented very well by the wave model, however the SWH is slightly underestimated overall, and the second, larger peak is not present in the modelled SWH. In addition, the model appears to decay on a slower scale than the observations. Overall, the modelled SWH appears smoother than the observed SWH. This is to be expected as the model represents an expected value of SWH over a 10 km by 10 km area, rather than a value at a single location.

Validation statistics are shown in Table 1. Although the rms error seems high when compared to a typical operational rms error of about 0.4 m, this is mainly due to the fact that the mean SWH here is high. The time-varying errors indicated by SI and R, show that the skill of the model in this case is very good. Note that a large portion of the bias and rms

Fig. 8 Comparison between SWH from the high-resolution wave model at (147.8°E, 38.5°S) (dashed line) and SWH measured at Kingfish B platform (solid line).



error here arises from the wave model not capturing the second peak in SWH. This is very similar to the pattern occurring in the wind speeds, i.e., the atmospheric model generally underpredicts wind speeds with most of the underestimation occurring during the second peak. From this, we may conclude that a large portion of the SWH bias is likely to be due to errors in the wind field.

One factor missing from the growth term within the wave model is the effect of the 'gustiness' in the wind, i.e., variability that occurs on time-scales shorter than the temporal resolution of the wind fields. Generally, gusts are defined to be random wind oscillations with periods of up to 20-30 minutes. In this study, new wind fields were provided at hourly intervals and so gusts are likely to be important here. This is particularly true since this is a situation of low static stability, which implies that there will be more turbulence in the atmosphere. It has been shown that variability or gustiness in the wind speed can enhance wave growth by up to 10 per cent (Komen et al. 1994), and so this could also help explain the underprediction in the modelled SWH.

To be able to completely explain the differences between the modelled and observed SWH, it would be necessary to compare total wave spectra. This would indicate at which frequencies and in which directions the wave model is lacking in energy, i.e., whether the deficiencies are in the swell or wind-sea components of the spectrum. However, observations of wave spectra are difficult to obtain and there were none available here during this time period.

One possible cause for underprediction of swell from the Tasman Sea storm is the 'sprinkler effect' (Booij and Holthuijsen 1987). This is due to poor res-

olution in the wave spectrum and causes the disintegration of swell energy as it propagates long distances across the ocean. This can eventually result in an unrealistic spatial distribution of swell energy from distant storms. In this study, the directional resolution of the wave spectrum has been doubled from the usual operational resolution in an attempt to minimise this effect.

Another possible source of error is the lack of current or depth refraction in the wave model. It has been shown, however, that depth refraction contributes very little to model performance statistics (Komen et al. 1994) and it is seldom included in operational wave models. As discussed earlier, the EAC may have some effect on the development of the sea-state by steepening the westerly propagating swell arising from the Tasman Sea storm. The effects of surface currents are not included in this study. It is not clear whether the potential alteration to this swell system would still be detected at the location of the KFB platform.

Yacht fleet reports

CYC99 presents summaries of some visual reports from competitors made in their post-race surveys. Although highly subjective, these reports do provide some interesting information that can be useful in a general examination of the sea-surface conditions.

The average wave height reported by the fleet was 9.4 m. This presumably was during the worst conditions that the boats encountered, and compares fairly well with the modelled SWH of 8.5 m. Assuming a Rayleigh distribution of waveheights, one might expect a maximum wave 1.91 times the SWH every 1500 waves. Assuming a peak period of nine seconds, this would therefore be encountered on average every 3.75 hours. Most of the fleet reported that they endured the most severe conditions for at least four hours, so according to the wave model, it would not be unusual for individual waves of over 15 m to be encountered. In fact, the average maximum wave height reported by the fleet was 14 m.

The yacht fleet reported that the direction of propagation of the waves was irregular, but that the average direction was 60°. This is consistent with the modelled sea-state depicted earlier, and particularly that shown in Fig. 6, where the mean wave direction is 68°. In addition, the yachts that experienced problems reported that 'exceptional' waves were responsible for causing knockdowns, and that these waves always came from a direction other than the prevailing wave pattern. This agrees with the idea of rogue waves, described previously.

Competitors in the race also commented that the 'waves had no back to them'. This effect is likely to be due to the steepening of the westerly-propagating swell by the EAC.

Conclusions

A high-resolution (0.1°) wave model has been run for the Bass Strait region over the period of the 1998 Sydney to Hobart yacht race. The maximum SWH reached in the wave model is 8.5 m, east of Gabo Island during the evening of 27 December. The model compares well with observations of significant wave height (SWH) at Kingfish B Platform in Bass Strait. There is an underprediction of SWH at this location of approximately 0.34 m. This is likely to be due to residual errors in the wind forcing fields. The wave model results are also consistent with visual observations of the sea-state made by competitors in the race.

Examination of the modelled ambient sea-state conditions and directional wave spectra during the race shows that in addition to the strong winds and high SWH experienced by the fleet, there were multiple wave systems present. At times, and particularly during the peak of the storm, these wave systems were propagating in almost opposite directions. This situation is termed 'crossing seas' and has the potential to create hazardous conditions for mariners.

Acknowledgments

The author wishes to thank George Cresswell for his comments on the EAC during the period of the yacht race and David Griffin for providing the gridded TP/ERS-2 surface velocity dataset. Thanks to Graham Mills for providing the wind fields used in this work and also to Rick Smith for providing the 0.1° bathymetric dataset. Lawson and Treloar provided the wave data from Kingfish B platform.

References

- Andrews, J.C. and Scully-Power, P.D. 1976. The structure of an East Australia Current anti-cyclonic eddy. *J. Phys. Oceanogr.*, 6, 756 - 65.
- Bender, L. 1996. Modification of the physics and numerics in a third-generation ocean wave model. *J. Atmos. Oc. Tech.*, 13, 726 - 50.
- Booij, N. and Holthuijsen, L.H. 1987. Propagation of ocean waves in discrete spectral wave models. *J. Comp. Phys.*, 68, 307 - 26.
- Bureau of Meteorology 1999. *Preliminary report on meteorological aspects of the 1998 Sydney to Hobart yacht race*. Bur. Met., Australia.
- Cardone, V.J., Jensen, R.E., Resio, D.T., Swail, V.R. and Cox, A.T. 1996. Evaluation of contemporary ocean wave models in rare extreme events: The 'Halloween Storm' of October 1991 and the 'Storm of the Century' of March 1993. *J. Atmos. Oc. Tech.*, 13, 198 - 230.
- Cruising Yacht Club of Australia. 1999. *Report of the 1998 Sydney to Hobart Race Review Committee*.
- Garratt, J.R. 1992. *The atmospheric boundary layer*. Cambridge Univ. Press, Cambridge, UK, 316pp.
- Greenslade, D.J.M. 2001. The assimilation of ERS-2 significant wave height data in the Australian region. *J. Mar. Sys.*, 28, 141-60.
- Gunther, H., Hasselmann, S. and Janssen, P.A.E.M. 1992. Wamodel Cycle 4, *DKRZ Report No. 4.*, Hamburg.
- Hasselmann, K., Barnett, T.P., Buows, E., Carlson, H., Cartwright, D.E., Enke, K., Ewing, J.A., Gienapp, H., Hasselmann, D.E., Kruseman, P., Meerburg, A., Muller, P., Olbers, D.J., Richter, K., Sell, W. and Walden, H. 1973. Measurements of wind-wave growth and swell decay during the Joint North Sea Wave Project (JONSWAP), *Dtsch. Hydrogr. Z. Suppl. A.*, 8(12), 95p.
- Komen, G.J. and Smith, N.R. 1999. Wave and sea level monitoring and prediction in the service module of the Global Ocean Observing System (GOOS). *J. Mar. Sys.*, 19, 235 - 50.
- Komen, G.J., Cavaleri, L., Donelan, M., Hasselmann, K., Hasselmann, S. and Janssen, P.A.E.M. 1994. *Dynamics and modelling of ocean waves*. Cambridge University Press, Cambridge, UK, 532 pp.
- Large, W.G. and Pond, S. 1981. Open ocean momentum flux measurements in moderate to strong winds. *J. Phys. Oceanogr.*, 11, 324 - 36.
- Mills, G. 2000. A Synoptic/diagnostic study of the 1998 Sydney-Hobart yacht race storm - a warm-cored extratropical cyclone. *BMRC Research Report No. 76*. Bur. Met., Australia
- Mills, G. 2001. Mesoscale cyclogenesis in reversed shear - the 1998 Sydney-Hobart yacht race storm. *Aust. Met. Mag.*, 50, 29-52.
- National Meteorological Operations Centre 1998. *Quarterly Summary, Oct - Dec 1998*. Bur. Met., Australia.
- National Meteorological Operations Centre 1999. The operational implementation of MESO_LAPS_PT125 in NMOC. *Operations Bulletin No. 49*. Bur. Met., Australia.
- Puri, K., Dietachmayer, G.S., Mills, G.A., Davidson, N.E., Bowen, R.A. and Logan, L.W. 1998. The new BMRC Limited Area Prediction System, LAPS. *Aust. Met. Mag.*, 47, 203 - 33.
- Seaman, R., Bourke, W., Steidle, P., Hart, T., Embery, G., Naughton, M. and Rikus, L. 1995. Evolution of the Bureau of Meteorology's Global Assimilation and Prediction System, Part 1: Analyses and Initialization. *Aust. Met. Mag.*, 44, 1 - 18.
- Swail, V., Komen, G., Ryabinin, V., Holt, M., Taylor, P.K. and Bidlot, J. 1999. Wind waves in the Global Ocean Observing System, in OCEANOBS99, *Proc. of the Int. Conf on the Ocean Observing System for Climate*, St. Raphael, France, 1999.
- Torum, A. and Gudmestad, O.T. (eds) 1990. *Water wave kinematics*. Kluwer Academic Publishers, Dordrecht, Holland, 771pp.

